PHYSICAL REVIEW A VOLUME 13, NUMBER 1 JANUARY 1976

Diabatic-states representation for He*($n \geq 3$) + He collisions*

James S. Cohen
Theoretical Division (T-6), Los Alamos Scientific Laboratory, University of California, Los Alamos, New Mexico 87544
(Received 2 June 1975)

A diabatic-states representation for scattering of triplet helium atoms, with $n \geq 3$, by the ground-state helium atom is presented. *Ab initio* calculations have been performed on the $^3\Sigma_{g,u}^+$, $^3\Pi_{g,u}$, and $^3\Delta_g$ Rydberg states of He_2. Matrix elements for radial and angular coupling between the orthogonalized diabatic states have also been evaluated. The angular couplings are quite weak, with the result that molecular states with different electronic symmetries are effectively uncoupled in low-energy collisions. The crossing by a repulsive diabatic-potential curve through the Rydberg series and into the continuum is shown to be an effective mechanism for associative ionization. Some qualitative observations on associative ionization and dissociative recombination are made.

I. INTRODUCTION

Collisions involving excited-state molecular-helium interactions provide interesting cases for interpretation in terms of both adiabatic and nonadiabatic potential curves. Among these processes are dissociative recombination, associative ionization (the Hornbeck-Molnar process[1]), and various inelastic excitation transfers. Although the complete set of adiabatic states is an adequate basis for a scattering calculation, it is now well known that these states do not necessarily provide a good physical picture of even low-energy collisions. However, a small number of linear combinations of these states can sometimes provide a more direct physical representation in which reasonable approximations to the scattering problem become evident.[2] Lichten[3] has shown that such states provide a simple explanation of experimental results for large-angle scattering in $He^+ + He$ resonant charge exchange, whereas the adiabatic-potential curves do not. The extreme case of the so-called "diabatic" states can be obtained by freezing the orbitals active in the collision in the form they have in the unperturbed atom. Sometimes it may be desirable to allow the diabatic orbitals to incorporate some effects of polarization or non-symmetry-breaking interactions, without permitting the drastic change of character occurring in the adiabatic wave functions.[4]

The Rydberg states of the He_2 molecule provide an especially simple case since the He_2^+ core has only two basic configurations, the attractive $1\sigma_g^2 1\sigma_u$, $^2\Sigma_u^+$, A core and the highly repulsive $1\sigma_g 1\sigma_u^2$, $^2\Sigma_g^+$, B core. The potential curves for the states of He_2, obtained by freezing the core and adding an electron in a frozen Rydberg orbital, are smooth and fall into two distinct classes, whereas the adiabatic-potential curves can be quite tortuous. Much experimental and theoretical work has been done to determine adiabatic-potential curves for the helium molecule,[5] and more recently interest has been aroused in nonadiabatic states. Previous work is suggestive of a diabatic mechanism for associative ionization and dissociative recombination in helium, but no quantitative evidence has been provided.

O'Malley,[6] motivated by the pronounced humps resulting from avoided crossings in some of the adiabatic curves of helium, has used the projected-orbital method to obtain a $^3\Pi_u$ $2p$ diabatic state of He_2. Guberman and Goddard[7] have calculated potential curves using frozen-orbital wave functions for the low-lying excited $^1\Sigma_{g,u}^+$ states of He_2. Steets and Lane[8] have inferred a $^3\Sigma_g^+$ $2s$ diabatic potential curve by smoothly joining different adiabatic curves. Description of the processes of associative ionization and dissociative recombination would require a large number of adiabatic states since, as Mulliken[9] has pointed out, no adiabatic state of He_2 crosses into the continuum delimited by the ground-state He_2^+ potential curve. That is, coupling between different adiabatic states must be large even for high Rydberg states. On the other hand, in the diabatic representation, states having the same core (A or B) tend to have parallel potential curves and to be only weakly coupled in collisions. Also, the coupling of a B-core curve at its crossings with a series of A-core curves will be shown to approach zero rapidly as the continuum limit is approached. Hence the diabatic states serve as a good basis for a finite-state scattering calculation.

In the present work a sufficiently complete set of diabatic states has been calculated to quantitatively demonstrate, using a simple scattering model, that the diabatic-states mechanism for associative ionization is a correct and straightforward interpretation.

Results for the $^3\Sigma_{g,u}^+$, $^3\Pi_{g,u}$, and $^3\Delta_g$ states are

presented in this paper. Diabatic wave functions and energies, in terms of which the scattering is interpreted, were first determined; then, configuration interaction between these states was allowed to derive the corresponding adiabatic states. The states were described by slightly generalized valence-bond–type wave functions. Each configuration is a sum of Slater determinants constructed to be an eigenfunction of the molecular symmetry operations and spin. The two He_2^+ curves were obtained using single configurations of elliptic orbitals with nonlinear parameters optimized at each internuclear distance. The core was then frozen and not allowed to adjust to the presence of an added outer electron. In the spirit of a diabatic description, the Rydberg electron was represented by a valence-bond orbital which was allowed to adjust at finite internuclear distances only to the extent required to preserve orthogonality among the different states. The mixing necessitated by the orthogonality constraint is quite small at intermediate distances ($R \gtrsim 2a_0$). The Rydberg orbitals were determined in separated-atom calculations and, in the case of non-S states, were found to be quite like hydrogenic orbitals. The resulting states form an orthogonal approximate diabatic set.

As discussed in the following paragraph, the derivative coupling between pairs of these states is expected to be small. Nevertheless, in the case of closely spaced Rydberg states this interaction may result in nonlocalized transitions, which are not expected to make much difference to associative ionization from low Rydberg states and are not taken into account at present. The possibility of describing states *within* each manifold (g or u core) adiabatically was considered but was decided against since the resulting states often do not satisfy the Massey criterion for adiabaticity; in any event, the scattering description is not expected to be strongly dependent upon this choice.

The nature of the coupling depends on the representation of the collision problem (adiabatic or diabatic basis, center-of-mass or separated-atom origin, space-fixed or body-fixed coordinates[10]) and can take the form of potential coupling (H_e), radial derivative coupling (d/dR), or angular derivative coupling ($d/d\Theta$ or $d/d\Phi$). By definition, there is no potential coupling between adiabatic states. The potential coupling among the calculated diabatic states is easy to obtain from the Hamiltonian matrix. A definition of the diabatic representation as one in which the radial derivative coupling vanishes has been attempted[11] but suffers some limitations.[12] In any event, the frozen-orbital states do not rigorously satisfy this criterion. The contribution to radial derivative coupling can nevertheless be expected to be small since the radial extent of the Rydberg orbital is usually large compared to the internuclear separation at which crossings between A- and B-core states occur; i.e., as the internuclear distance changes, the change in the orbital relative to either nucleus is small and hence the radial derivative has been neglected. Angular couplings, known to be important for $2s \rightarrow 2p$ inelastic transitions in helium scattering,[13] have been calculated and shown to be negligible compared to radial couplings for states with principal quantum numbers $n \geq 3$. Hence the complexity of many scattering calculations, including those involving ionization or recombination, can be reduced since only the set of states which are connected by potential coupling need be considered.

Calculations of cross sections using the diabatic representation are presented in the following paper. Some features, such as the vibrational and electronic excitation levels of the collision reactants and products in dissociative recombination and associative ionization, can easily be estimated by just examining the potential curves and coupling matrix elements in the diabatic representation, and are discussed in this paper.

II. CORES FOR THE RYDBERG STATES

The non-s Rydberg orbitals of the helium atom are, to a good approximation, hydrogenic with unit nuclear charge (the exception of s orbitals is discussed in Sec. III A). Since the maximum charge of the main lobe of a hydrogenic orbital occurs at about $n(n-1)a_0$, a frozen atomic Rydberg orbital attached to an unperturbed He_2^+ core should be a good approximation to the molecular Rydberg states formed from $n \geq 3$ atoms, at least for internuclear distances where the interaction is appreciable. The present calculations required He_2^+ wave functions which were simple but still yielded accurate potential curves. Simplicity was dictated by the need for large numbers of Rydberg states, and accuracy of the potential curves avoids the necessity of empirical and somewhat arbitrary energy adjustments. Wave functions which met these criteria nicely were of the type

$$\psi = |\phi_{AB}(0,0,0)^2 1s'_B| \pm |\phi_{BA}(0,0,0)^2 1s'_A| , \qquad (1)$$

where ϕ_{AB} and ϕ_{BA} are elliptic (prolate-spheroidal) orbitals, $1s'_A$ and $1s'_B$ are Slater-type orbitals (STO), A and B label the two nuclear centers, the vertical bars designate Slater determinants, and the + and − signs yield states of $^2\Sigma_g^+$ and $^2\Sigma_u^+$ symmetry, respectively. The elliptic orbitals are

defined by[14]

$$\phi_{AB}(n,l,m) = (2\pi)^{1/2}(-1)^{(|m|-m)/2}\xi^n\eta^l \times[(\xi^2-1)(1-\eta^2)]^{|m|/2} \times e^{-\delta\xi-\gamma\eta}e^{im\varphi}, \quad (2)$$

where $\xi=(r_A+r_B)/R$ and $\eta=(r_A-r_B)/R$ at internuclear distance R, and where φ is the azimuthal angle about the internuclear axis. The result of the inversion operator on ϕ_{AB} is $\phi_{BA}=(-1)^m\phi_{AB}$ ($\delta\to\delta$, $\gamma\to-\gamma$). It may be noted that for $\delta=\pm\gamma$ the orbitals are centered on the nuclei, and for $\gamma=0$ the orbitals are centered at the midpoint of the molecule. In the separated-atom limit $\phi(0,0,0)$ has the property of becoming a 1s STO located on center A or B, with nonlinear parameter $2\delta/R = \pm 2\gamma/R = 1.6875$ for He. The He^+ STO is primed to indicate that it has a different nonlinear parameter, $\alpha=2.0$, in the separated-atom limit. The nonlinear parameters were optimized at each internuclear separation, but the 1s' orbital changed negligibly. Near the equilibrium position ($R\simeq 2.0a_0$), the optimized parameters of the elliptic orbital for the $^2\Sigma_u^+$ state are $2\delta/R=1.82$ and $2\gamma/R=\pm 1.63$. At the same distance the optimized parameters for the $^2\Sigma_g^+$ state are $2\delta/R=1.73$ and $2\gamma/R=\pm 1.68$. As expected, more charge moves toward the center of the molecule in the case of the bonding state.

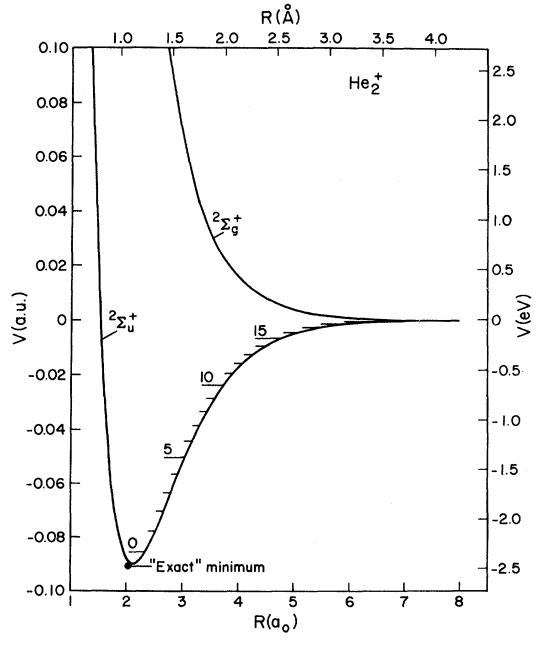

FIG. 1. Calculated potential curves for He_2^+. The vibrational levels in the ground state are shown. The point labeled "exact minimum" is the result of a calculation by Liu (Ref. 15).

The resulting potential curves are shown in Fig. 1. The $^2\Sigma_u^+$ ground-state potential curve is in quite good agreement, undoubtedly somewhat fortuitously, with the very accurate configuration-interaction calculation of Liu.[15] A well depth of 2.424 eV was obtained as compared to Liu's best value of 2.469 ± 0.006 eV. The 20 vibrational levels determined by analysis of the calculated curve using Numerov integration are also shown in Fig. 1. The $^2\Sigma_g^+$ potential curve is in good agreement with the configuration-interaction calculation of Gupta and Matsen[16] at $R\geq 2a_0$. At $R\lesssim 1.5a_0$ this curve is not a good approximation to the true adiabatic curve, as there is a series of avoided crossings[3,17] arising from configurations not included in the wave function, Eq. (1). However, this region is of little concern in the present low-energy applications since the repulsion of the potential at such short internuclear separations ($\gtrsim 19$ eV) is much greater than the ionization potential of the lowest excited state of the helium atom (<5 eV); i.e., the He*+He scattering system would have to stay on a repulsive diabatic curve high into the continuum in order to be affected.

Perhaps some justification is appropriate for the optimization of nonlinear parameters of the elliptic orbitals which were used in the cores of otherwise frozen-orbital wave functions. The core electrons, which have a lower principal quantum number and see a larger effective nuclear charge, have much higher velocities than the Rydberg electrons and hence tend to be more adiabatic in behavior. Furthermore, the change in the orbital exponents with internuclear distance is gradual, and in the energy range of interest here there are no curve crossings.

III. EXCITED MOLECULAR STATES OF He_2

A. Rydberg orbitals

As already discussed, the molecular Rydberg orbitals are quite similar to the corresponding separated-atom Rydberg orbitals except for the effects of avoided crossings and orthogonality constraints. In the case of non-S states, the atomic Rydberg orbitals were taken to be hydrogenic; for the convenience of using standard integral routines, these were expanded in terms of STO's,

$$\phi(n,l,m) = \sum_{k=l+1}^{n} \frac{(-1)^{k-l-1}}{(k-l-1)!\,(n-k)!\,(k+l)!} \times\left(\frac{(n-l-1)!\,(2k)!\,(n+l)!}{2n}\right)^{1/2} S(k,l,m), \quad (3)$$

with the usual definition of a STO with orbital parameter α,

$$S(k,l,m) = \frac{(2\alpha)^{3/2}}{[(2k)!\,]^{1/2}} (2\alpha r)^{k-1} e^{-\alpha r} Y_l^m(\theta, \varphi).$$

The maximum error in the binding energy of the Rydberg electron relative to He^+ (or, equivalently, the ionization energy of the Rydberg state) was 2.5% and occurred in the lowest-lying ^3P state.[18] The relative errors in the higher ^3P states are smaller, and the errors in states of higher orbital angular momenta are negligible (less than 0.1% for the ^3D states and of spectroscopic accuracy for the ^3F, ^3G, and ^3H states). In the case of S states, hydrogenic orbitals are a poor approximation to the Rydberg orbitals because they are not orthogonal to the 1s core orbital. Consequently a six-configuration atomic calculation, with configurations $1s'\,ns$, $1 \leq n \leq 6$, where $1s'$ and ns are STO's, was performed. Rather than applying the variational principle in the usual way to minimize the lowest root with respect to the nonlinear parameters, the sum of the lowest five roots was minimized, yielding orthogonal approximations for the n^3S, $2 \leq n \leq 6$ states from a single basis set (the ground state is automatically orthogonal to this set since it is a singlet). The maximum error in the binding energy of the s Rydberg electron was less than 1%.

The molecular wave functions formed by the interaction of a ground-state atom with the above excited states are orthogonal in the separated-atom limit but become nonorthogonal at finite distances as the spherical symmetry is broken. The diabatic states must be made orthogonal for the potential curves and couplings to be meaningful in a scattering calculation. Since the nonorthogonality is weak at intermediate distances, the Gram-Schmidt procedure is sensible. The states were orthogonalized in the order of increasing asymptotic energy and the resulting transformation was applied to the Hamiltonian matrix. Testing showed that the potential-energy curves and couplings were not sensitive to the order in which the states were orthogonalized.

B. Potential curves

Calculations were performed on five different molecular symmetries: $^3\Sigma_g^+$, $^3\Sigma_u^+$, $^3\Pi_g$, $^3\Pi_u$, and $^3\Delta_g$. The primary interest of these calculations was in the crossing of diabatic potential energy curves. Diabatic Rydberg states built on the $He_2^+\ ^2\Sigma_u^+$ core are attractive, and those built on the $He_2^+\ ^2\Sigma_g^+$ core are repulsive (except possibly for long-range dispersion minima). That is, states formed from even-l Rydberg atoms (s, d, etc.) are attractive if the molecular symmetry is ungerade and repulsive if the molecular symmetry is gerade, and vice versa for states formed from odd-l Rydberg atoms (p, f, etc.). In the cases of $^3\Sigma_u^+$ and $^3\Pi_g$ symmetries the lowest diabatic molecular states are attractive and undergo no crossings with other diabatic potential curves of like symmetry; for this reason, the $^3\Sigma_u^+$ 2s and $^3\Pi_g$ 2p, 3p configurations[19] were excluded from the calculations. All repulsive (B-core) configurations dissociating to atomic states with principal quantum number $n \leq 4$ were

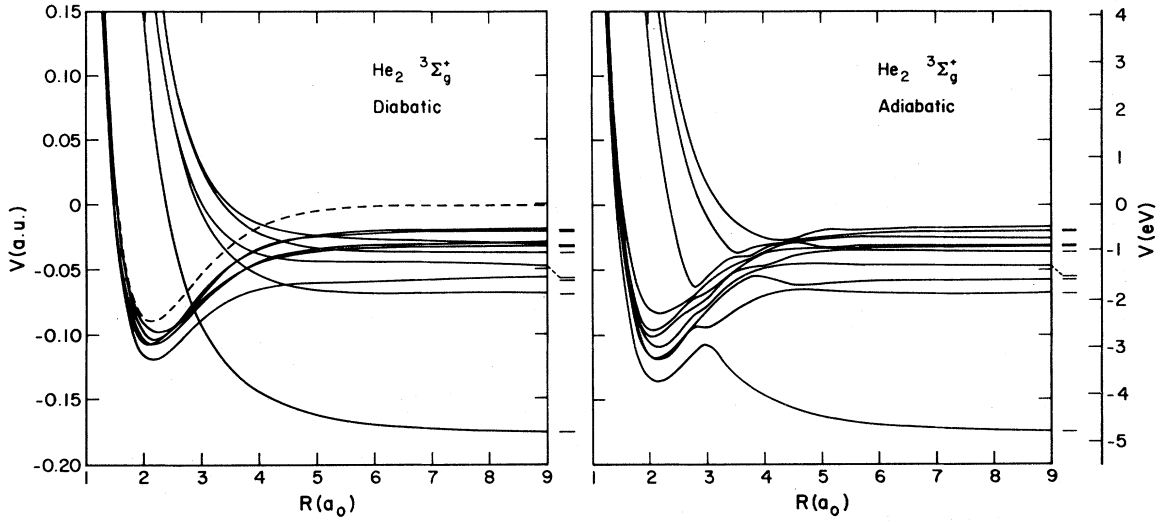

FIG. 2. Diabatic and adiabatic He_2 potential curves of $^3\Sigma_g^+$ symmetry. The dashed curve, representing the continuum limit, is the ground state of He_2^+ (from Fig. 1). The potential energy is measured relative to the separated-atom energy of $He^+ + He$. The designated separated-atom limits are 2s, 3s, 3p, 3d, 4s, 4p, 4d, 4f, 5p, and 5f.

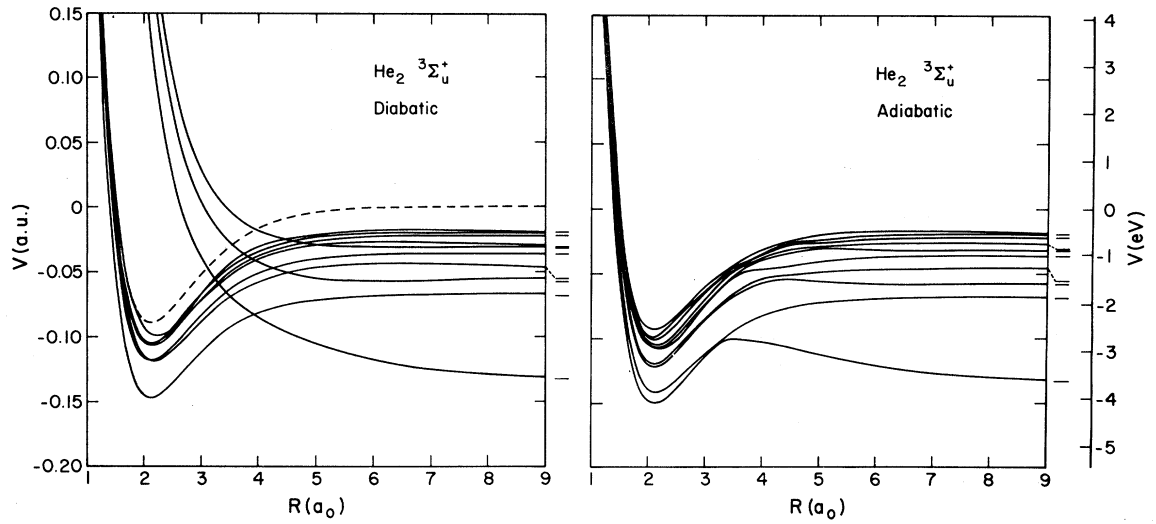

FIG. 3. Diabatic and adiabatic He_2 potential curves of $^3\Sigma_u^+$ symmetry. The designated separated-atom limits are $2p$, $3s$, $3p$, $3d$, $4s$, $4p$, $4d$, $5s$, $5d$, and $5g$.

included. All attractive configurations with $n \leq 6$ for the Σ and Δ states and $n \leq 5$ for the Π states were included except for the three noted above.

The diabatic potential curves, resulting from orthogonalization of the zero-order configurations, are shown in Figs. 2–6. The adiabatic states obtained by diagonalizing the Hamiltonian matrix (the off-diagonal elements are discussed in Sec. IV A) are shown for comparison in Figs. 2–6 and can be seen to possess much structure due to avoided curve crossings. The interpolation of the adiabatic potential curves between *ab initio* calculations was actually carried out by interpolating the smoother diabatic curves and off-diagonal elements of the Hamiltonian matrix and diagonalizing at each point. The higher states which appear to cross into the He_2^+ continuum are not good approximations to the true adiabatic states since only a finite number of valence-bond configurations were taken into account. It should be pointed out that the present "adiabatic" $^3\Sigma_u^+$ and $^3\Pi_g$ potential curves are not rigorous upper bounds since some low-lying configurations were excluded. The continuum limit of the attractive Rydberg states is shown as a dashed line. The vibrational levels near the crossings into the continuum can be identified in Table I.

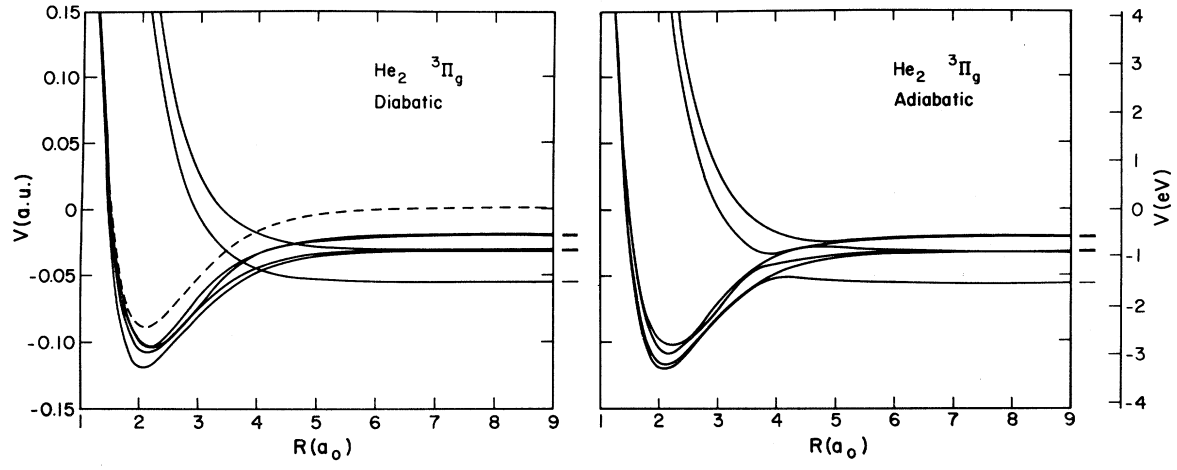

FIG. 4. Diabatic and adiabatic He_2 potential curves of $^3\Pi_g$ symmetry. The designated separated-atom limits are $3d$, $4p$, $4d$, $4f$, $5p$, and $5f$.

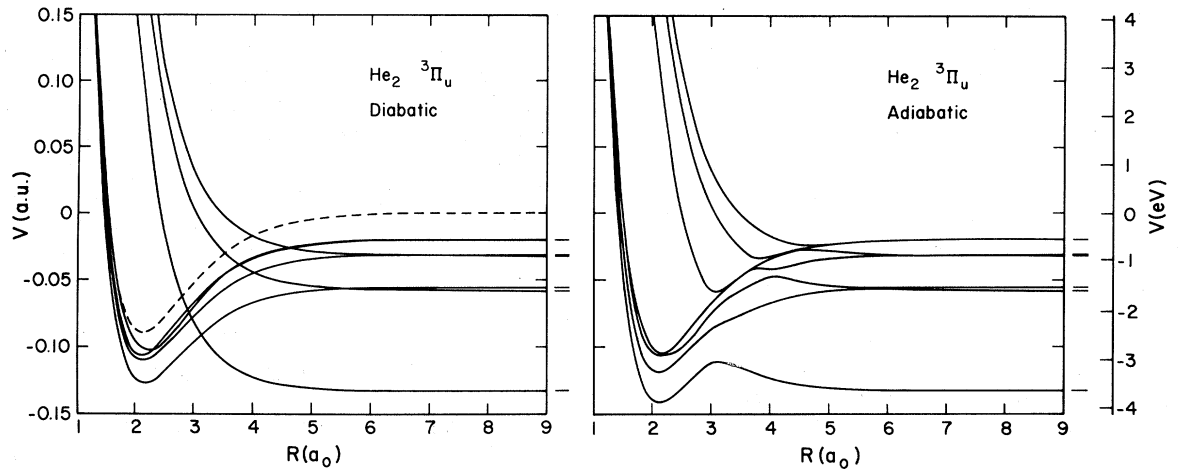

FIG. 5. Diabatic and adiabatic He_2 potential curves of $^3\Pi_u$ symmetry. The designated separated-atom limits are $2p$, $3p$, $3d$, $4p$, $4d$, $5d$, and $5g$.

Within a given molecular symmetry, the diabatic-potential curves follow separate Rydberg series for states formed from each atomic l quantum number (ns, np, etc.), having in common the limits of the $^2\Sigma_u^+$ and $^2\Sigma_g^+$ potential curves of He_2^+. Generally, the dissociation energies of the A-core states are smallest for the lowest Rydberg states of the series and increase toward the He_2^+ dissociation energy as n increases. These differences in well depths result in some very-small-angle crossings between different A-core potential curves at small to intermediate internuclear separations. In most of these cases the resulting adiabatic curves are so close together compared to the vibrational-energy–level spacings that it may be better to view the effect as homogeneous perturbation of the vibronic-rotational levels associated with the diabatic curves rather than as avoided crossing between the adiabatic curves.[20] The crossings between the A-core and B-core states all occur outside the minimum of the molecular-ion ground-state potential curve. The lowest crossing of a B-core state potential curve with the ground-state curve of He_2^+ is 1.80 eV below the He_2^+ dissociation energy for the $^3\Sigma_g^+$ states, 1.28 eV for $^3\Sigma_u^+$, 0.86 eV for $^3\Pi_g$, 1.70 eV for $^3\Pi_u$, and 0.79 eV for $^3\Delta_g$. The crossings of A- and B-core–state potential curves arising from atomic levels with different principal quantum numbers occur with large crossing angles. Crossings be-

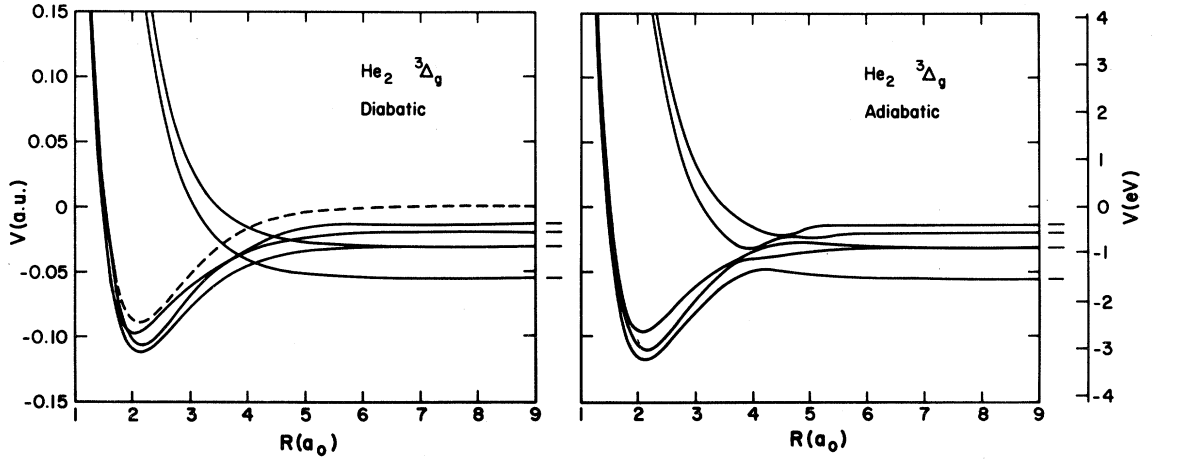

FIG. 6. Diabatic and adiabatic He_2 potential curves of $^3\Delta_g$ symmetry. The designated separated-atom limits are $3d$, $4d$, $4f$, $5f$, and $6f$.

tween potential curves arising from the same n quantum level tend to occur at large distances and with small crossing angles, with this tendency increasing as n increases and the atomic energies get closer together.

Small potential barriers occur in most of the diabatic states of Σ symmetry. The existence of such humps, termed "nonobligatory" by Mulliken,[9] has been well documented.[7,21] In most cases the humps which arise independently of any curve crossing are significantly smaller in the adiabatic curves, being reduced by the potential coupling with nearby diabatic states. One exception is the $^3\Sigma_u^+$ $3d$ state, which has a quite high barrier, about 0.3 eV in the diabatic and adiabatic potential curves. It can also be observed that the $^3\Sigma_g^+$ $3d$ potential is quite repulsive at large distances. This behavior can be understood as follows: The repulsive long-range potential results from the exchange forces which tend to exclude electron probability of the excited atom from the closed-shell ground-state atom (these forces should not be confused with Van der Waals forces which may result in attraction at still larger distances). The greatest effect should occur when the maximum charge extends toward the ground-state atom. This is achieved by the Σ state with the highest angular momentum which is possible with a principal quantum number that is still low enough that the charge is not too radially diffuse. That is, for potential curves arising from $n=2,3,4,\ldots$, the strongest long-range repulsion is expected in the $\Sigma\,2p, \Sigma\,3d, \Sigma\,4f,\ldots$ states, respectively, by the first criterion; it turns out that $n=3$ best satisfies the two criteria simultaneously. As also predicted by the above argument, the non-Σ states exhibit very small or no potential barriers.

IV. COUPLING MATRIX ELEMENTS

A. Radial coupling

The radial coupling, connecting diabatic states of the same electronic symmetry, is mainly potential coupling, $V_{12}(R)$, i.e., owing to the off-diagonal matrix elements of the electronic Hamiltonian. For example, the R-dependent matrix elements coupling the repulsive $2s$, $3s$, and $3d$ states of $^3\Sigma_g^+$ symmetry to several attractive A-core $^3\Sigma_g^+$ states are shown in Figs. 7, 8, and 9, respectively. The parameters for these and other radially coupled curve crossings are given in Table II. The convergence of the matrix element $\langle nl|H_e|n'l'\rangle$ toward zero as n' increases for given n, l, and l', with $n'>n$, is apparent. Also, for

TABLE I. A. Calculated vibrational levels of ground-state He_2^+. B. Energies and internuclear distances of crossings of repulsive diabatic curves with the He_2^+ potential curve.

A		B		
v	E_v (eV)[a]	State	E_x (eV)[a]	R_x (a_0)
0	0.107	$^3\Sigma_g^+$ $2s$	0.63	2.74
1	0.315	$3s$	1.48	3.41
2	0.514	$3d$	1.64	3.58
3	0.705	$4s$	1.89	3.91
4	0.887	$4d$	1.99	4.07
5	1.059			
6	1.222	$^3\Sigma_u^+$ $2p$	1.14	3.12
7	1.376	$3p$	1.63	3.56
8	1.520	$4p$	1.94	3.98
9	1.654			
10	1.779	$^3\Pi_g$ $3d$	1.56	3.49
11	1.893	$4d$	1.94	3.98
12	1.997			
13	2.091			
14	2.173	$^3\Pi_u$ $2p$	0.72	2.81
15	2.245	$3p$	1.60	3.53
16	2.305	$4p$	1.95	4.00
17	2.354			
18	2.390	$^3\Delta_g$ $3d$	1.64	3.57
19	2.414	$4d$	1.97	4.03

[a] Energies relative to minimum of He_2^+ potential curve. $D_e=2.424$ eV.

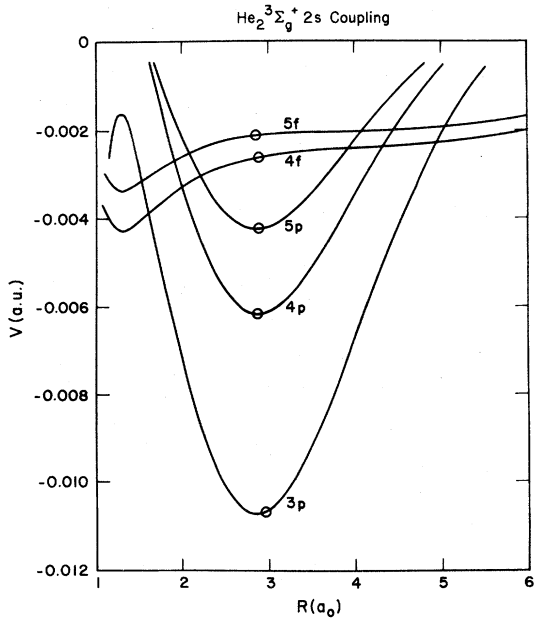

FIG. 7. Potential coupling of the repulsive $^3\Sigma_g^+$ $2s$ diabatic state to the attractive p and f states of that symmetry. The curve-crossing points are circled.

given n, l, and n', with $n' > n$, the coupling tends to decrease as $|l' - l|$ increases. The coupling at the lowest diabatic curve crossing in He_2, between the $^3\Sigma_g^+ 2s$ and $^3\Sigma_g^+ 2p$ states, has previously been shown to be quite large.[22]

To obtain an idea of how the matrix elements V_{12} are reflected in transition probabilities for jumping from one diabatic curve, V_{11}, to another, V_{22}, at the crossing distance R_x, consider the Landau-Zener (LZ) formula[23]

$$p = e^{-2\pi\gamma}, \tag{4}$$

where

$$\gamma = \gamma_r = \frac{|V_{12}(R_x)|^2}{\hbar v_R(R_x)\,|(d/dR)(V_{11} - V_{22})|_{R=R_x}} \tag{5}$$

at the velocity satisfying

$$\tfrac{1}{2}\mu v_R(R_x)^2 = E - V_{11}(R_x) - (l + \tfrac{1}{2})^2/2\mu R_x^2 . \tag{6}$$

It is easy to demonstrate that convergence with increasing n is rapid. Consider the crossing undergone by a repulsive diabatic state with the members of a Rydberg series arising from higher principal quantum number atomic states, say $n \geq 3$. Suppose that the coupling decreases as $n^{-3/2}$ and that the slopes of the potential curves and the effective velocities are all about the same.[24] With these assumptions and taking typical values for a thermal-energy collision, suppose the LZ parameter is given by $\gamma_n = 5/n^3$. [For example, at the crossing velocity corresponding to the collision He $*(3\,^3P)$+He at an asymptotic energy of 0.027 eV with $l = 0$, the formula derived from the parameters in Table II for the $2s$-$6p$, $^3\Sigma_g^+$ crossing is $4.3/n^3$, and the behavior of $V_{12}(2s\text{-}np,\ ^3\Sigma_g^+)$ for n this large is very nearly $n^{-3/2}$.] Then the probability of crossing through curves $n = 3, 4, \ldots, N$,

$$P_N = \exp[-2\pi(\gamma_3 + \gamma_4 + \cdots + \gamma_N)] , \tag{7}$$

is given by 0.31 for $N = 3$, 0.19 for $N = 4$, 0.13 for $N = 6$, 0.10 for $N = 10$, and 0.09 as $N \to \infty$.

It may be noted in Figs. 7–9 that some of the potential-coupling matrix elements have extrema and zeros. This structure can be shown to be related to the nodal structure of the Rydberg orbitals. At sufficiently large internuclear distances, the matrix elements all decay exponentially, as expected. The orthonormalization procedure slightly changes the couplings quantitatively but does not alter the basic nodal structure. In a two-state calculation it is easy to show that the smallest energy gap between two adiabatic curves which have an avoided crossing is twice the potential coupling between the zero-order configurations at their crossing point. This relation is still sometimes useful in determining effective couplings even in multiconfiguration calculations. However, in the case of the excited He_2 potential curves, the crossings are generally too close together to isolate a particular pair of diabatic curves. The long-range

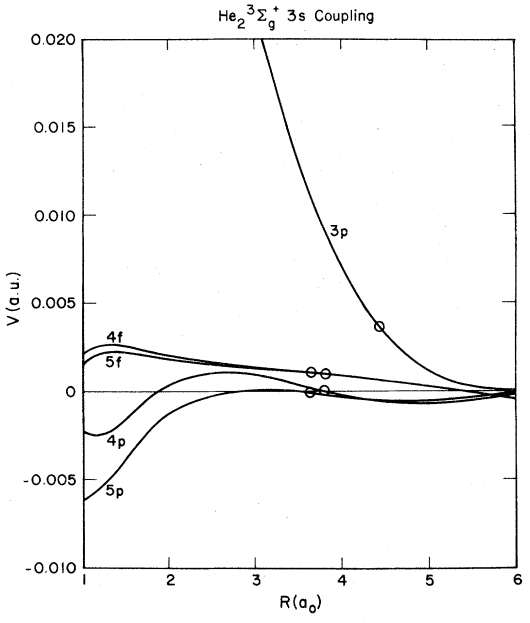

FIG. 8. Potential coupling of the repulsive $^3\Sigma_g^+$ $3s$ diabatic state to the attractive p and f states of that symmetry. The curve-crossing points are circled.

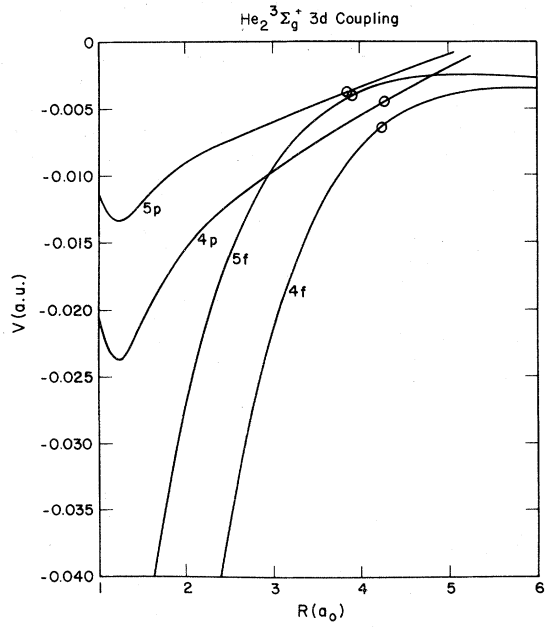

FIG. 9. Potential coupling of the repulsive $^3\Sigma_g^+$ $3d$ diabatic state to the attractive p and f states of that symmetry. The curve-crossing points are circled.

TABLE II. Parameters for radially coupled diabatic-curve crossings.[a]

States	R_x	$E(R_x)$[b]	$\Delta\left(\frac{dV}{dR}\right)_{R_x}$	$V_{12}(R_x)$
		$^3\Sigma_g^+$		
$2s$-$3p$	2.96	−0.0902	0.1336	−1.07 E − 2
-$4p$	2.85	−0.0795	0.1524	−6.19 E − 3
-$4f$	2.88	−0.0817	0.1527	−2.59 E − 3
-$5p$	2.85	−0.0788	0.1619	−4.24 E − 3
-$5f$	2.83	−0.0768	0.1690	−2.11 E − 3
-$6p$	2.77	−0.0693	0.1778	−3.04 E − 3
-$6f$	2.77	−0.0699	0.1648	−1.55 E − 3
$3s$-$3p$	4.45	−0.0616	0.0160	3.59 E − 3
-$4p$	3.79	−0.0490	0.0505	8.01 E − 5
-$4f$	3.79	−0.0490	0.0526	1.03 E − 3
-$5p$	3.61	−0.0431	0.0714	−1.30 E − 4
-$5f$	3.61	−0.0432	0.0660	1.06 E − 3
-$6p$	3.54	−0.0404	0.0630	1.62 E − 5
-$6f$	3.60	−0.0428	0.0650	8.44 E − 4
$3d$-$4p$	4.29	−0.0409	0.0194	−4.52 E − 3
-$4f$	4.25	−0.0405	0.0221	−6.48 E − 3
-$5p$	3.87	−0.0356	0.0406	−3.82 E − 3
-$5f$	3.90	−0.0362	0.0369	−4.12 E − 3
-$6p$	3.84	−0.0350	0.0343	−2.78 E − 3
-$6f$	3.88	−0.0357	0.0424	−2.69 E − 3
$4s$-$4p$	5.37	−0.0345	0.0053	−4.85 E − 4
-$4f$	5.10	−0.0336	0.0086	2.61 E − 5
-$5p$	4.38	−0.0281	0.0211	5.35 E − 4
-$5f$	4.41	−0.0285	0.0226	−3.25 E − 4
-$6p$	4.36	−0.0278	0.0262	5.04 E − 4
-$6f$	4.28	−0.0267	0.0343	−3.50 E − 4
$4d$-$4f$	8.29	−0.0290	0.0017	−2.30 E − 3
-$5p$	5.13	−0.0244	0.0066	−8.89 E − 4
-$5f$	4.99	−0.0239	0.0099	−2.68 E − 3
-$6p$	4.74	−0.0277	0.0188	−1.12 E − 3
-$6f$	4.57	−0.0215	0.0225	−2.09 E − 3
		$^3\Pi_g$		
$3d$-$4p$	4.09	−0.0467	0.0341	−1.19 E − 3
-$4f$	4.00	−0.0452	0.0360	−6.51 E − 3
-$5p$	3.77	−0.0406	0.0542	−8.69 E − 4
-$5f$	3.75	−0.0399	0.0499	−3.57 E − 3
$4d$-$4f$	>10	...	...	...
-$5p$	4.71	−0.0268	0.0128	−7.06 E − 4
-$5f$	4.67	−0.0265	0.0154	−1.96 E − 3
		$^3\Delta_g$		
$3d$-$4f$	4.13	−0.0437	0.0339	−4.97 E − 3
-$5f$	3.86	−0.0380	0.0470	−2.98 E − 3
-$6f$	3.84	−0.0374	0.0517	−1.88 E − 3
$4d$-$4f$	8.75	−0.0313	4.3 E − 5	−1.50 E − 6
-$5f$	4.76	−0.0261	0.0150	−1.59 E − 3
-$6f$	4.48	−0.0235	0.0278	−1.23 E − 3
		$^3\Sigma_u^+$		
$2p$-$3s$	3.93	−0.0833	0.0471	3.05 E − 3
-$3d$	3.53	−0.0695	0.0716	−3.06 E − 2
-$4s$	3.45	−0.0660	0.0794	−3.04 E − 3
-$4d$	3.33	−0.0599	0.0902	−1.87 E − 2
-$5s$	3.30	−0.0587	0.0941	2.44 E − 3
-$5d$	3.25	−0.0555	0.1064	−1.31 E − 2
-$5g$	3.26	−0.0563	0.0977	−4.04 E − 4
-$6s$	3.24	−0.0549	0.0996	−2.17 E − 3
-$6d$	3.18	−0.0513	0.0974	−9.97 E − 3
-$6g$	3.24	−0.0553	0.0988	−3.86 E − 4
$3p$-$3d$	4.52	−0.0511	0.0218	−4.39 E − 3
-$4s$	4.26	−0.0475	0.0265	2.41 E − 3
-$4d$	3.96	−0.0417	0.0442	−9.59 E − 3
-$5s$	3.91	−0.0404	0.0470	−1.10 E − 3
-$5d$	3.77	−0.0364	0.0563	−6.64 E − 3
-$5g$	3.84	−0.0385	0.0508	−1.69 E − 5
-$6s$	3.78	−0.0369	0.0555	6.90 E − 4
-$6d$	3.77	−0.0365	0.0502	−4.66 E − 3
-$6g$	3.77	−0.0366	0.0602	−9.79 E − 5
$4p$-$4d$	5.04	−0.0296	0.0095	−4.78 E − 4
-$5s$	4.80	−0.0283	0.0143	−1.63 E − 3
-$5d$	4.47	−0.0254	0.0195	−3.35 E − 3
-$5g$	4.61	−0.0267	0.0181	6.78 E − 6
-$6s$	4.43	−0.0249	0.0239	1.25 E − 3
-$6d$	4.42	−0.0248	0.0280	−2.31 E − 3
-$6g$	4.33	−0.0238	0.0294	1.53 E − 5
		$^3\Pi_u$		
$2p$-$3d$	3.14	−0.0916	0.1029	−1.91 E − 2
-$4d$	2.97	−0.0791	0.1317	−9.87 E − 3
-$5d$	2.93	−0.0751	0.1500	−6.26 E − 3
-$5g$	2.91	−0.0729	0.1482	−2.37 E − 4
$3p$-$3d$	5.64	−0.0568	0.0035	1.91 E − 4
-$4d$	4.04	−0.0450	0.0372	−4.23 E − 3
-$5d$	3.78	−0.0388	0.0532	−2.97 E − 3
-$5g$	3.80	−0.0394	0.0509	5.50 E − 5
$4p$-$4d$	6.34	−0.0319	0.0016	3.88 E − 5
-$5d$	4.68	−0.0265	0.0149	−1.57 E − 3
-$5g$	4.66	−0.0263	0.0171	4.37 E − 5

[a] All quantities in atomic units.

[b] Relative to $He^+ + He$ separated-atom energy.

crossings which tend to occur between molecular states arising from the same principal quantum level are an exception. For these relatively flat crossings, long-range polarization effects, reflected in the adiabatic potentials, tend to reduce the effective coupling. The coupling matrix elements deduced from the adiabatic potentials in these cases are given in Table III. These modified matrix elements may be better representations of the effective coupling in a two-state approximation or in a model where transitions are assumed to occur only in narrow regions around the curve crossings. In a complete treatment, e.g., converged close coupling, such modifications are of course unnecessary.

B. Angular coupling

In addition to the radial coupling between states of like symmetry, there is angular coupling, of the form $\Omega_{12} = \langle \psi_1 | L_y | \psi_2 \rangle$, between electronic states whose components of angular momentum along the internuclear axis differ by ± 1, e.g., Σ and Π, Π and Δ, etc. (The z axis is taken along the internuclear line and the y axis perpendicular to the plane of the collision.) This coupling has been shown to be the dominant source of inelastic transitions between the $1s2s$ and $1s2p$ states of helium,[13] since the corresponding radial potential coupling is so large that the particles tend to follow the adiabatic curves.[22] In fact, the very strong mixing of $2p$ character into the $^3\Sigma$ $2s$ adiabatic state results in the unusually large angular-coupling matrix element. The mixing is not nearly as strong for higher states, and the angular coupling for those adiabatic states does not exceed that for the corresponding diabatic states by nearly so much. In general, both types of coupling tend to become weaker as n increases. Hence it is not unexpected that for $n \geq 3$ the radial coupling becomes the main source of inelasticity and the angular coupling ceases to be important; this behavior is illustrated in the last paragraph of this section.

The crossing parameters for some of the angularly coupled diabatic states are given in Table IV. The matrix element of L_y was calculated in the body-fixed, geometrical-center-of-the-nuclei (GCN) system, which is the same as the body-fixed, center-of-mass-of-the nuclei (CMN) system

TABLE III. Effective radial-potential coupling for long-range crossings, derived from adiabatic-potential curves.[a]

States	R_x	$V_{12}(R_x)$
$^3\Sigma_g^+$ $3s$-$3p$	4.63	2.01 E−3
$4s$-$4p$	5.37	5.2 E−4
$4d$-$4f$	8.5[b]	2.8 E−3[b]
$^3\Pi_g$ $4d$-$4f$	11.3	1.38 E−6
$^3\Delta_g$ $4d$-$4f$	9.49	2.09 E−6
$^3\Sigma_u^+$ $3p$-$3d$	4.39	8.8 E−4
$4p$-$4d$	5.1	8.0 E−4
$^3\Pi_u$ $3p$-$3d$	6.02	1.38 E−4
$4p$-$4d$	6.72	2.87 E−5

[a] All quantities in atomic units.
[b] No minimum was found in $V_{11}(R) - V_{22}(R)$, but the function does have an inflection point at which these values were determined.

TABLE IV. Parameters for angularly coupled diabatic-curve crossings.[a]

States	R_x	$E(R_x)$[b]	$\Delta\left(\frac{dV}{dR}\right)_{R_x}$	$\Omega_{12}(R_x)$
		$^3\Sigma_g^+$-$^3\Pi_g$		
$2s$-$3p$	3.09	−0.1014	0.1236	−2.67 E−2
-$4p$	2.92	−0.0861	0.1466	−2.09 E−2
-$4f$	2.88	−0.0823	0.1522	2.93 E−3
$3s$-$3p$	4.65	−0.0636	0.0170	−1.40 E−1
-$4p$	3.87	−0.0514	0.0500	2.02 E−2
-$4f$	3.80	−0.0493	0.0521	−1.27 E−3
$3d$-$4p$	4.41	−0.0417	0.0192	−1.27 E−2
-$4f$	4.28	−0.0407	0.0213	2.43 E−1
$4s$-$4p$	5.43	−0.0346	0.0054	1.19 E−1
-$4f$	5.18	−0.0339	0.0074	−1.93 E−4
$4p$-$3d$	3.99	−0.0451	0.0344	−1.89 E−2
$4f$-$3d$	3.98	−0.0449	0.0367	1.69 E−1
-$4d$	6.13	−0.0309	0.0023	3.23 E−3
		$^3\Pi_g$-$^3\Delta_g$		
$3d$-$4f$	4.02	−0.0456	0.0357	−3.93 E−3
$4d$-$4f$	8.10	−0.0313	0.0001	2.56 E−5
$4p$-$3d$	4.20	−0.0448	0.0325	4.07 E−2
$4f$-$3d$	4.11	−0.0433	0.0342	−1.03 E−1
		$^3\Sigma_u^+$-$^3\Pi_u$		
$2p$-$3d$	3.66	−0.0747	0.0612	3.38 E−1
-$4d$	3.38	−0.0626	0.0852	1.61 E−1
$3p$-$3d$	5.47	−0.0572	0.0048	2.07 E−3
-$4d$	4.08	−0.0443	0.0378	1.84 E−1
$4p$-$4d$	6.43	−0.0318	0.0005	−1.87 E−3
$3s$-$2p$	3.29	−0.1004	0.0882	−1.08 E−1
$3d$-$2p$	3.06	−0.0864	0.1168	1.92 E−1
-$3p$	4.50	−0.0513	0.0203	2.77 E−3
$4s$-$2p$	3.02	−0.0832	0.1259	4.81 E−2
-$3p$	4.23	−0.0480	0.0292	1.08 E−1
$4d$-$2p$	2.94	−0.0761	0.1372	9.33 E−2
-$3p$	3.92	−0.0425	0.0439	1.08 E−1
-$4p$	5.12	−0.0292	0.0088	−1.38 E−5

[a] All quantities in atomic units.
[b] Relative to He^+ + He separated-atom energy.

for the homonuclear molecule. At small to intermediate internuclear separations, the angular coupling calculated in this system can sometimes be used in a two-state approximation to obtain inelastic cross sections. At large and very small distances, however, the interaction of the particles is not strong enough to make the eigenfunctions follow the rotation of the internuclear line during the collision.[25] Coupling between states with $\Delta\Lambda = \pm 1$ then reflects the fact that the initial state with quantum number Λ in body-fixed coordinates becomes, in general, a linear combination of $2J+1$ possible values of Λ as a result of an elastic collision. The large-distance behavior of the L_y matrix element in body-fixed GCN coordinates is easy to determine. Writing the wave functions in the valence-bond form (the actual wave functions employed are somewhat generalized),

$$\psi_i = (1/\sqrt{2})(\chi_a\phi_{ib} \pm \chi_b\phi_{ia}), \quad i = 1 \text{ or } 2, \tag{8}$$

where χ is the He ground-state wave function and ϕ_1 and ϕ_2 are the initial and final excited atomic wave functions, the matrix element is

$$\Omega_{12} = \langle \chi_a\, \phi_{1b} \,|\, L_y \,|\, \chi_a\, \phi_{2b}\rangle \pm \langle \chi_a\, \phi_{1b} \,|\, L_y \,|\, \chi_b\, \phi_{2a}\rangle \ , \tag{9}$$

where L_y is a sum over the operators L_{y_j} for each electron j. The operator L_{y_j} can conveniently be written

$$\frac{i\hbar R}{2}\frac{\partial}{\partial x_{ja}} + (L_{y_j})_a \quad \text{or} \quad \frac{i\hbar R}{2}\frac{\partial}{\partial x_{jb}} + (L_{y_j})_b \tag{10}$$

for electrons associated with atom a or b, respectively, where

$$x_a = -x, \quad y_a = y, \quad z_a = -z - \tfrac{1}{2}R$$

and

$$x_b = x, \quad y_b = y, \quad z_b = z - \tfrac{1}{2}R\,.$$

Neglecting the exponentially decreasing contribution owing to the identical nuclei, the asymptotic form is

$$\Omega_{12} \sim (1/2i)\langle \phi_{1b} \,|\, (L_+)_b - (L_-)_b \,|\, \phi_{2b}\rangle + \tfrac{1}{2}R\langle \phi_{1b} \,|\, i\hbar \sum_{j\in b} \frac{\partial}{\partial x_{jb}} \,|\, \phi_{2b}\rangle \ , \tag{11}$$

where L_y has been written in terms of the raising and lowering operators, and the fact that none of the operators have nonzero matrix elements with χ has been used. The matrix element in the second term is just the integral which appears in the velocity form of the electric dipole transition moment; thus the coupling given in the second term is proportional to R in the asymptotic limit if the transition between ϕ_1 and ϕ_2 is dipole allowed. Since the atomic states are orthogonal, the contribution due to the first term approaches a constant in the asymptotic limit, which is nonzero provided the states ϕ_1 and ϕ_2 differ merely by $|\Delta M| = 1$ where M is the magnetic quantum number. This coupling is a characteristic of body-fixed coordinates. The R-proportional coupling does not appear in the separated-atom (SA) coordinate system, but the SA system has other inconvenient coupling terms at short to intermediate distances.[10] Hence either a transformation from CMN to SA coordinates or an arbitrary cutoff of the R-proportional coupling (with sensitivity checks) in the course of the outward integration will often be expedient.

Most of the angularly coupled crossings in He_2 occur at sufficiently small R that a two-state treatment may still be possible with the matrix element calculated in the CMN system. The coupling will be assumed for the present discussion to be localized, although this is a fairly difficult condition to fulfill in the case of angular coupling,[26] particularly for long-range crossings. Applying the LZ approximation, Eq. (5) is replaced by

$$\gamma_a = \frac{|\,\omega(R_x)\Omega_{12}(R_x)\,|^2}{\hbar v_R(R_x)\,|\,(d/dR)(V_{11}-V_{22})|_{R=R_x}}\,, \tag{12}$$

where

$$\omega(R_x) = (l+\tfrac{1}{2})/(\mu R_x^2)\,. \tag{13}$$

To demonstrate, as previously claimed, that the angular coupling is negligible in slow collisions with the excited atom in a state $n \geq 3$, consider, as an example, the inelastic collision

$$\mathrm{He}(2\,^3S) + \mathrm{He} \rightarrow \mathrm{He}(3\,^3P) + \mathrm{He}\ .$$

The ratio of the angular-coupling to radial-coupling parameters is

$$\frac{\gamma_a}{\gamma_r} \simeq \left(\frac{\omega(R_x)\Omega_{12}(R_x)}{V_{12}(R_x)}\right)^2 = (l+\tfrac{1}{2})^2\left(\frac{\Omega_{12}(R_x)}{\mu R_x^2 V_{12}(R_x)}\right)^2 \simeq 5.8\times 10^{-9}(l+\tfrac{1}{2})^2\,, \tag{14}$$

implying that $l \simeq 13\,000$, or $E \gtrsim 72$ keV, is required for the two to be comparable. Since γ_a and γ_r are in or close to the weak-coupling region, defined by $\exp(-2\pi\gamma) > 0.5$, this means that the angular coupling in Table IV is largely ineffective in slow collisions.

V. DISCUSSION

A quantitative diabatic-states picture of the Rydberg states of He_2 has been presented with emphasis on the potential-curve crossings. The calculations have been carried out for the triplet states

only, but similar results for the singlets may be expected. In the following paper[27] cross sections for associative ionization and inelastic excitation transfer are obtained using this representation. Remarks here will be limited to a few qualitative observations on associative ionization and its inverse process, dissociative recombination.

It has been experimentally observed that the recombination rate in helium-afterglow plasmas is unusually low and seems not to proceed by dissociative mechanisms.[28-30] To reconcile this fact with the observation of large cross sections for associative ionization it has been postulated that He_2^+ must be vibrationally excited for dissociative recombination to occur.[9] Some $2\,^3P$ atoms apparently resulting from dissociative recombination have been observed spectroscopically,[29] consistent with the small fraction of ions in excited vibrational states, and $2\,^3S$ metastables have not been ruled out.

It may be seen from Table I that $2\,^3P$ atoms can be expected to result from $^3\Pi_u$ dissociation if He_2^+ is vibrationally excited to $v \gtrsim 4$ and from $^3\Sigma_u^+$ dissociation for $v \gtrsim 6$. The level $v=4$ at 0.89 eV, corresponding to $(E_4 - E_0)/k \simeq 9000$ °K, is only very slightly populated in the usual helium-afterglow experiment. It may also be seen from Table I that $2\,^3S$ or $2\,^3P$ atoms may result from $^3\Sigma_g^+$ dissociation for $v \gtrsim 3$. On the other hand, dissociation into higher (triplet) atomic states would require a quite high vibrational excitation of the molecular ion ($v \gtrsim 8$ or higher). As is clear from the potential curves of Figs. 2–6, as well as required by the principle of detailed balance, any He_2^+ molecular ion resulting from associative ionization will be vibrationally excited.

A well-documented experimental observation about associative ionization in helium is that the process has a quite small cross section at thermal energies for the $3\,^{1,3}S$ states,[31] even though their excitation energies are greater than $E_i(\mathrm{He}) - E_d(\mathrm{He}_2^+)$, where $E_i(\mathrm{He})$ is the ionization potential of the He atom and $E_d(\mathrm{He}_2^+)$ is the dissociation energy of He_2^+. This observation has been interpreted as implying that there are no accessible crossings into the continuum in these collisions. This conclusion appears to be confirmed by the present calculations—the repulsive $^3\Sigma_u^+\ 2p$ and $^3\Pi_u\ 2p$ curves, which are radially and angularly coupled, respectively, to the attractive $^3\Sigma_u^+\ 3s$ curve, do cross the He_2^+ curve at energies somewhat higher than the $3\,^3S$ excitation energy. However, even if one or both of these crossings into the continuum were energetically accessible, the theory still predicts that the cross sections would be very small at thermal energies. Basically this is because resistance to the crossing of the $^3\Sigma_u^+\ 2p$ state through the Rydberg series of attractive states is unusually large, and the fact that angular coupling of the $^3\Sigma_u^+\ 3s$ to the $^3\Pi_u\ 2p$ state is very weak as discussed in Sec. IV; quantitative discussion will be deferred to the following paper.

ACKNOWLEDGMENT

A computer program of the molecular physics group, The University of Texas at Austin, was modified for the potential-curve and matrix-element calculations.

---

*Work performed under the auspices of the U.S. Energy Research and Development Administration.

[1]J. A. Hornbeck and J. P. Molnar, Phys. Rev. 84, 621 (1951).
[2]T. F. O'Malley, Adv. At. Mol. Phys. 7, 223 (1971).
[3]W. Lichten, Phys. Rev. 131, 229 (1963).
[4]H. S. Taylor (private communication).
[5]M. L. Ginter and R. Battino, J. Chem. Phys. 52, 4469 (1970), and references therein.
[6]T. F. O'Malley, J. Chem. Phys. 51, 322 (1969).
[7]S. L. Guberman and W. A. Goddard III, Chem. Phys. Lett. 14, 460 (1972).
[8]W. J. Steets and N. F. Lane (private communication); Phys. Rev. A 11, 1994 (1975).
[9]R. S. Mulliken, Phys. Rev. 136, A962 (1964).
[10]R. T Pack and J. O. Hirschfelder, J. Chem. Phys. 49, 4009 (1968).
[11]F. T. Smith, Phys. Rev. 179, 111 (1969).
[12]H. Gabriel and K. Taulbjerg, Phys. Rev. A 10, 741 (1974).
[13]L. Lenamon, J. C. Browne, and R. E. Olson, Phys. Rev. A 8, 2380 (1973); E. J. Shipsey, J. C. Browne, and R. E. Olson, Phys. Rev. A 11, 1334 (1975).
[14]F. E. Harris and H. S. Taylor, J. Chem. Phys. 38, 2591 (1963); J. C. Browne, J. Chem. Phys. 40, 43 (1964).
[15]B. Liu, Phys. Rev. Lett. 27, 1251 (1971).
[16]B. K. Gupta and F. A. Matsen, J. Chem. Phys. 47, 4860 (1967).
[17]J. C. Browne, J. Chem. Phys. 45, 2707 (1966).
[18]C. E. Moore, *Atomic Energy Levels*, Natl. Bur. Stand. Circ. No. 467 (U.S. GPO, Washington, D.C., 1949), Vol. I.
[19]Separated-atom orbital designations are used throughout this paper; this notation is especially convenient for diabatic states.
[20]R. S. Mulliken, J. Am. Chem. Soc. 88, 1849 (1966).
[21]J. C. Browne, J. Chem. Phys. 42, 2826 (1965).
[22]S. A. Evans, J. S. Cohen, and N. F. Lane, Phys. Rev. A 4, 2235 (1971).
[23]L. Landau, Phys. Z. Sowjetunion 2, 46 (1932); C. Zener, Proc. R. Soc. A 137, 696 (1932); E. C. G. Stueckel-

berg, Helv. Phys. Acta 5, 369 (1932).
[24]The probability given by Eq. (7) will in fact converge to a nonzero value as long as the coupling decreases faster than $n^{-1/2}$. The $n^{-3/2}$ dependence of the matrix element $\langle n'l'|H_e|nl\rangle$ (the core electrons are left implicit in this notation), where $n \gg n'$ and $n \gg l$, is easy to understand. The highly excited electron is well described by a hydrogenic wave function. Provided that $n \gg l$, the hydrogenic eigenfunction depends on n simply as $n^{-3/2}$ in the region $r \ll n^2$ [see H. A. Bethe and E. E. Salpeter, *Quantum Mechanics of One- and Two-Electron Atoms* (Springer–Verlag, Berlin, 1957), p. 18]. The last inequality is satisfied since the exponential asymptotic form of the $n'l'$ function cuts off the contribution to the off–diagonal matrix element at large r [in particular, at $r \gtrsim \bar{r}(nl)$]. In the example given in the text ($2s$–np, $^3\Sigma_g^+$) the $n^{-3/2}$ behavior holds at rather small n. In other cases involving more diffuse (n' larger) and/or less penetrating (l' larger) orbitals, this dependence is not apparent until rather higher n.
[25]D. R. Bates, Proc. R. Soc. A 240, 437 (1957); 243, 15 (1957); 245, 299 (1958); in *Atomic and Molecular Processes*, edited by D. R. Bates (Academic, New York, 1962), p. 597.
[26]A. Russek, Phys. Rev. A 4, 1918 (1971).
[27]J. S. Cohen, following paper, Phys. Rev. A 13, 99 (1976).
[28]E. E. Ferguson, F. C. Fehsenfeld, and A. L. Schmeltekopf, Phys. Rev. 138, A 381 (1965).
[29]W. W. Robertson, J. Chem. Phys. 42, 2064 (1965); C. B. Collins and W. W. Robertson, J. Chem. Phys. 43, 4188 (1965).
[30]G. K. Born, Phys. Rev. 169, 155 (1968).
[31]H. F. Wellenstein and W. W. Robertson, J. Chem. Phys. 56, 1077 (1972).